VOL. 9, NO. 10, OCTOBER 2014 ISSN 1819-6608
ARPN Journal of Engineering and Applied Sciences

www.arpnjournals.com

USE OF A SOUND SOURCE LOCALISATION SYSTEM FOR THE EXPERIMENTAL DETERMINATION OF VIBRATION PATTERNS OF A SQUARE PLATE

Jürgen Göken, Henning Arends and Hans Brink
Faculty of Maritime Studies, University of Applied Sciences Emden/Leer, Bergmannstr. 36, 26789 Leer, Germany
E-Mail: juergen.goeken@hs-emden-leer.de

ABSTRACT

It is well known that there are only a few non-contact methods to localise sound and vibration sources. Keeping noise due to vibration on a low level is a very important matter, not only for passenger shipping companies but also for maritime classification societies like the Germanischer Lloyd (GL). Own measurements have shown that vibrations caused by ship´s structure occur primarily at the windows of a ship. The noise caused by these vibrating windows turned out to be a very significant sound source that can be disturbing for crew and - especially on passenger ships - for passengers. In order to visualise the sound field and to accomplish an accurate localisation of the vibration amplitudes occurring in an acrylic glass square pane which was excited into vibration a sound source localisation system (Microflown™ probe) including a USB camera was used. The experiment was performed at excitation frequencies of 20 Hz, 30 Hz and 50 Hz. Additionally, the influence of different mountings and shifting of the position of the device (lifting magnet) for initiation of vibrations were investigated. The received data were compared with Chladni figures that developed under the same experimental conditions.

Keywords: sound, noise measurements, Microflown™, maritime technology, Chladni figure.

1. INTRODUCTION

The comfort for passengers of transport vehicles like e.g. cars, trains, airplanes and ships will always be scaled down as long as structure-borne noise reaches a sound level that disturbs human wellness. The frequencies appearing on vessels are dependent on several factors. These factors are the ship´s speed, the structure of the ship´s hull and the material it is made of, the external voyage conditions (e.g. weather, tide, state of the sea), but most important is the propulsion. Acoustic measurements with common microphones are much less significant to big, slow operating main engines that lead to quite low oscillation frequencies on board. The Germanischer Lloyd (GL) defines vibration on board as “Structural oscillations in the frequency range of 1 to 80 Hz” (GL [1]) and is one of several classification societies that deal with the influence of structural oscillations on the comfort of passengers. It is pointed out that “Notations of comfort, obviously, needed particular attention for passenger ships” (Asmussen *et al.*, [2]). According to this classification societies began their own investigations about vibrations and comfort, first on passenger vessels and in a next step on other ships. The GL illustrated annoyance due to vibrations so considerable that it calls itself “the first Classification Society to base the vibration part on the new ISO 6954 standard” (Asmussen *et al.*, [2]).

The windows of a ship are of special interest concerning the acoustic emission. Own measurements have shown the localised noise from vibrating windows of a passenger vessel (Figure-1). The area colour-coded in red means a high sound pressure whereas the blue colour-coded area represents a low sound pressure. It can be confirmed that the sound radiation of the windows constitute a comfort problem.

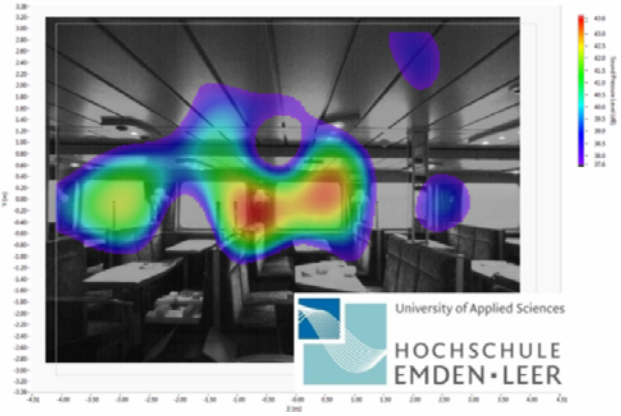

Figure-1. Visualised sound pressure of vibrating windows of a passenger vessel (Göken [3]).

For the laboratory measurement of an oscillating plate that shall simulate a vibrating window of a ship the ability of measuring low-frequency sound waves with low vibration amplitudes is highly important, especially when clamping conditions have to be considered. Conventional microphones are designed to measure the sound pressure caused by the changing sound waves, whereas the used sensor (Microflown™ probe) with pressure and particle velocity microphones is able to determine the particle motion of the air directly. To do so, two tiny platinum wires are heated up to 200 °C. The sound wave in the air forces the air molecules to flow past these wires at different rates and initiate a cooling process. Due to this different cooling the electrical resistances of the wires change. This change of resistance generates a voltage difference that is proportional to the particle velocity. By using the Microflown™ probe it is possible to detect

vibrations within a frequency range between 0.1 Hz - 20.0 kHz (Table-1) very accurately.

Table-1. Acoustical properties of the Microflown™ probe (Microflown™ [4]).

	frequency range	**upper sound level**	**polar pattern**	**directivity**
sound pressure sensor	20 Hz - 20 kHz	110 dB	omnidirectional	omnidirectional
particle velocity sensor	0.1 Hz - 20 kHz	125 dB	figure of eight	directive

The motion of a plate is analogous to a two-dimensional beam or membrane with internal shear and bending resistance. Membranes and plates can emit sound because of vibrations which are caused by simple hammering. While a membrane has to be clamped to get into vibration the thickness of a plate is responsible for the bending elasticity and the ability to oscillate. A lot of extensive studies about the vibration of classical plates for various shapes, boundaries and loading conditions have been made for nearly two centuries. The analysis methods for vibrations of plates are analytical, numerical and experimental whereas both the analytical and the numerical method suffer from accuracy when complicated shapes or various boundary conditions have to be considered (Ma and Lin, [5]). The use of experimental methods is sometimes lengthy but helpful to find the vibration pattern of membranes or plates, especially the nodal lines.

Chladni [6] drew attention to the extremely large variety of vibration possibilities of plates. He made the nodal lines visible by sprinkling sand on them (so called "Chladni figures"): The sand is thrown off the moving regions and piles up at the nodes. One possibility to create Chladni figures is to draw the about the middle on a tripod horizontally mounted plate at the edge in the vertical direction with a violin bow. The simultaneously holding of one or more boundary points with the fingers can lead to different modes of vibration. Figures-2(a) to (e) are given as examples for sound patterns of a square metal plate. The plates were excited at the point marked b to oscillate and held at the points marked with k. Two adjacent parts of the plate, separated by a nodal line, vibrate always in the opposite direction perpendicular to the plane of the plate. As seen in Figure-2 different sound patterns can arise. The plate is bowed until it reaches resonance and the sand forms a pattern showing the nodal regions.

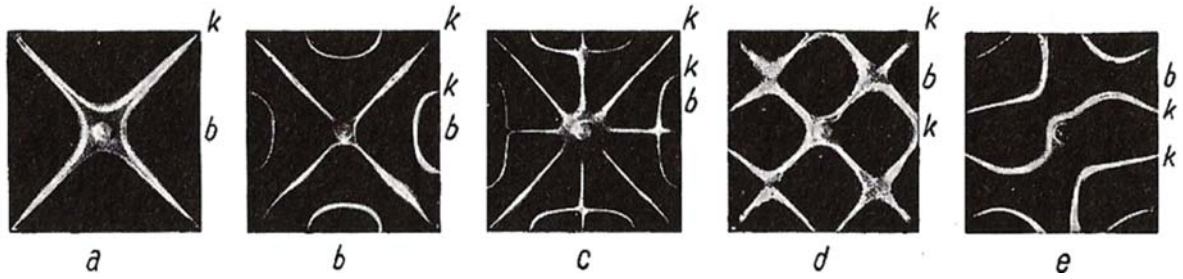

Figure-2. Chladni figures of a square plate (Bergmann *et al.*, [7]).

Generally, there are different types of boundaries considered for a plate in terms of lateral deflection of the middle surface of the plate. They are: a) clamped edge conditions, b) simply supported edge conditions, c) mixed edge conditions and d) free edge conditions (Balasubramanian [8]). If a plate is clamped at the boundary, then the deflection and the slope of the middle surface must completely vanish at the boundary. The problem of transverse vibration of a rectangular or square plate clamped at all four edges is one of the most important and interesting characteristic-value problems in elastokinetics (Tomotika [9]). An established work on the calculation of vibration modes of differently shaped plates was written by Leissa [10]. Various boundary conditions (e.g. all sides clamped of a rectangular plate) are shown and discussed in his compendium.

The present work will show the results of acoustic measurements performed on an acrylic glass square pane which was excited into vibrations by an external force. In order to get an impression of the developing vibration pattern the nodal lines were made visible by creating the Chladni figures. A comparison between the Chladni figures and the results of the acoustic measurements is carried out.

2. MATERIALS AND METHODS

2.1 Experimental setup

The experimental setup for the measurements is shown in Figure-3. By changing the clamping conditions its influence on the nodal development was investigated.

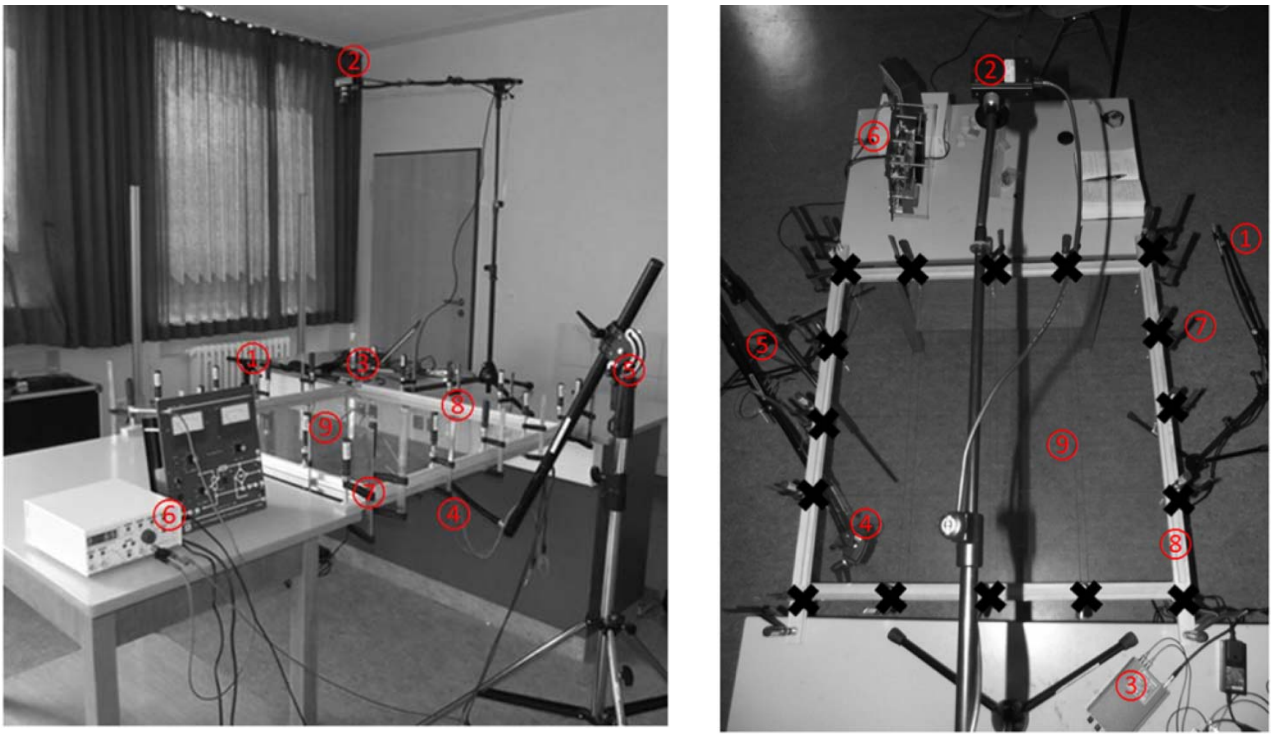

Figure-3. Experimental setup. The numbers are described in the text.

A square acrylic glass pane with an edge length of 1 m and a thickness of 2 mm (9) was fixed within a frame of wooden laths (8). The frame being positioned parallel to the basement was held tight by 16 bar clamps (7) that were firmly tightened. The bar clamps were positioned in equidistant distances of 0.25 m. The detailed mounting scheme of the acrylic glass pane is shown in Figure-4. Two different kinds of wooden laths were used in order to raise the distribution of the contact pressure caused by the bar clamps.

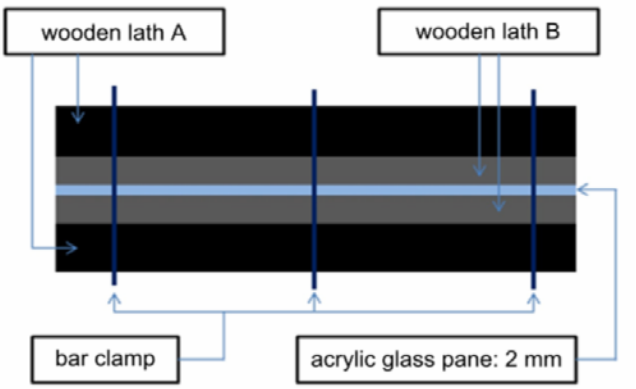

Figure-4. Mounting scheme of the acrylic glass pane.

Beneath the acrylic glass pane an electric hammering device including a lifting magnet (4) was mounted. By connecting this device to voltage an internal electromagnetic field was created which attracted the lifting magnet. When the voltage was switched off the magnet sprang back to its original position by using a spring. A frequency generator (6) allowed changing the frequency of the attraction procedure. When the lifting magnet of the electric hammering device sprang back it hammered against the acrylic glass pane which started to oscillate. Three different excitation frequencies (20 Hz, 30 Hz and 50 Hz) were used during the experiment. Measurements with a frequency of 20 Hz have also been repeated under different experimental conditions which will be discussed later. While the lifting magnet beat against the acrylic glass pane it was supposable that it would push itself away from the pane. To avoid this, a firm mounting device (5) consisting of a tripod, a clamping tool and a strong flex arm was applied.

The sound source localisation system consisted of a Microflown™ probe (1), a signal converter (3) and a USB camera (2). All acoustic measurements were analysed by using the CAE™ software "Intensity Inspector" (version 3.2). The Chladni figures were produced before the acoustic measurements were carried out in order to estimate the nodal lines of the acrylic glass pane. These lines could be visualised after sprinkling fine-grained sand on the surface of the pane whereas it had to be ensured that only a thin layer of sand was present. For comparison of the results of the Chladni figures and the sound source localisation system all measurements were executed under identical clamping, excitation and meteorological conditions (air temperature: 23 °C, humidity: 60 %).

2.2. Experimental conditions for determination of the Chladni figures

The visualisation of the nodal lines due to distribution of the sand is a continuous process and was stopped after a hammering period of 30 minutes. By changing some experimental conditions like reducing the number of bar clamps (Figure-5), by laying weights on top of the acrylic glass pane (Figure-6) and by changing the position of the lifting magnet (Figure-12) it should be clarified how intensely these changes influence the vibration pattern. Figure-5 shows the experimental setup with reduced clamping. The four red crosses mark the missing bar clamps while the black ones represent those that were not removed. The aim of this procedure was to lower the compacting pressure in one part of the acrylic glass pane. The lifting magnet has not been moved and stayed at its original position in the center of the pane.

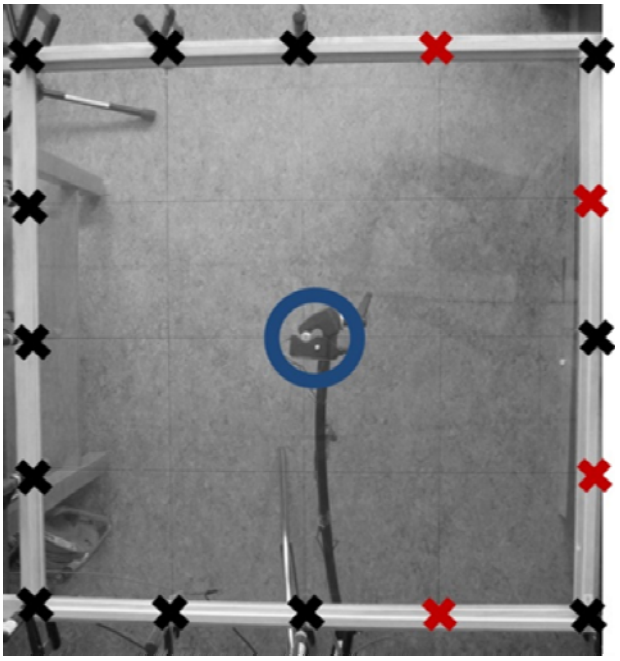

Figure-5. Reduced clamping (missing bar clamps are marked by a red cross).

In Figure-6 all bar clamps were set on their previous position and stoutly set tight. Before the motion of the lifting magnet was activated two pieces of steel (each weight: 250 g) had been laid on top of the acrylic glass pane. The blue circle marks the position of the lifting magnet while the positions of the steel weights are marked by the two yellow circles. The lifting magnet beat against the pane with a frequency of 20 Hz. After removing the weights the lifting magnet was positioned at the lower right corner of the acrylic glass pane. The results of this experiment which was carried out at 20 Hz are shown in Figure-12.

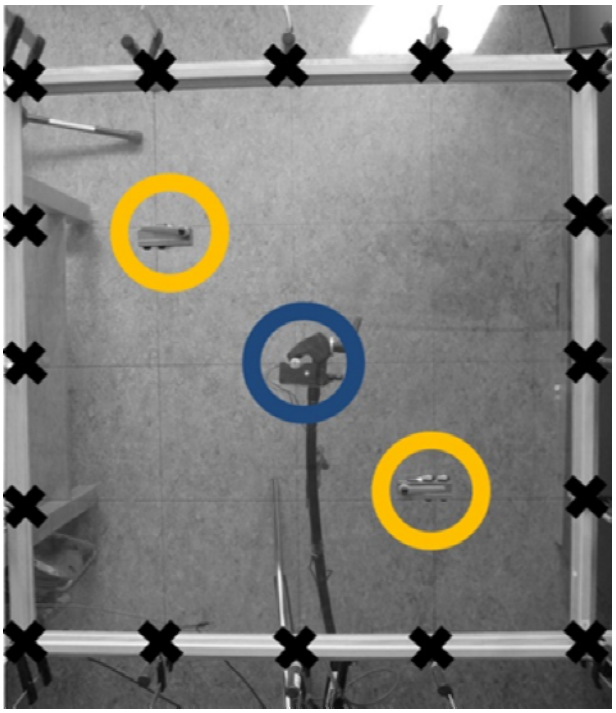

Figure-6. Additional weights (located in the yellow circles) on the surface of the acrylic glass pane.

2.3. Experimental conditions for determination of the particle velocity using a Microflown™ probe

After development of the Chladni figures the sand was removed from the pane and the Microflown™ probe was used to demonstrate another way of detecting vibrations. The following procedures for data acquisition have been executed as follows: At first a measurement plane has to be defined which is represented by the surface of the acrylic glass pane acting as the sample. Afterwards a USB camera is applied to take a digital picture of the sample from a fixed distance that must not be changed during the measurements. Due to the limited measuring area of the Microflown™ probe checkpoints on the pane have to be defined. The shorter the distance between these points the more accurate is the expected information about the vibration behaviour. In the fixed vertical distance above these checkpoints the Microflown™ probe has to be aligned and records data within a prior defined time frame. A software processes the data and relates them to each other to visualise the vibration activity at each checkpoint by colour-coding. As an example in Figure-7 the sound pressure produced by an oscillating bending beam fixed at one is illustrated. The strongest movement at the free end of the bending beam could be confirmed. Due to the low excitation frequency and the broader frequency range of the particle velocity sensor (Table-1) the structure-born noise was measured in terms of the particle velocity instead of the sound pressure.

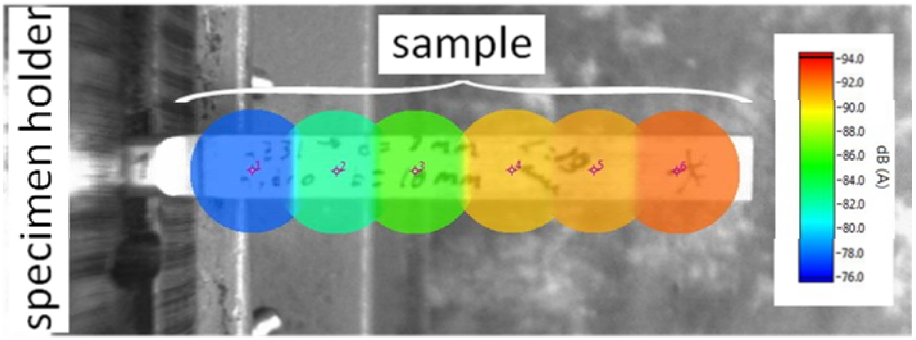

Figure-7. Sound emission measurement of an oscillating bending beam. The colour-coded areas represent the local oscillation amplitude leading to an individual sound pressure. Red color: high sound pressure, blue color: low sound pressure (Göken *et al.*, [11]).

In order to receive representative results about the acrylic glass pane vibration 81 checkpoints have been marked on the pane in equidistant distances of 10 cm. The acrylic glass pane was set under continuous excitation by the lifting magnet. While the pane was oscillating the Microflown™ probe was positioned in a vertical distance of 1 cm above every single checkpoint and collected data over a period of three seconds per checkpoint. The particle velocity for each checkpoint was measured. Due to the dense concentration of measuring points the sound field of the complete acrylic glass pane could be received. The data of each point were set in relation to each leading to a colour-coded map which was laid over the digital picture of the acrylic glass pane with the Chladni figure that was created before. This digital picture was taken by the USB camera from a distance of 1.2 m above the pane.

3. RESULTS AND DISCUSSIONS

3.1. Vibrational states of plates

Ventsel and Krauthammer [12] wrote a remarkable overview of the mathematical methods for the description of the vibrational states of plates. Their work serves as a basis in this paper for the physical considerations that are relevant in the description of square plate vibrations. In the following discussion about vibration of plates the effect of damping by internal friction or the surrounding media is neglected. Although structural damping is theoretically present in all plate vibrations, it has usually little or no effect on the natural frequencies and the steady-state amplitudes (Ventsel and Krauthammer, [12]).

The governing differential equation for deflection of plates in cartesian coordinates is given as

$$\frac{\partial^4 w}{\partial x^4} + 2\frac{\partial^4 w}{\partial x^4 \partial y^4} + \frac{\partial^4 w}{\partial y^4} = \nabla^2\left(\nabla^2 w\right) = \frac{p}{D}, \qquad (1)$$

where $w(x,y)$ is the deflection function, $p(x,y)$ is the distributed load of intensity and $D = \frac{Eh^3}{12(1-\nu^2)}$ is the flexural rigidity of the plate with h as the thickness of the plate, E the modulus of elasticity, ν the Poisson's ratio and ∇^2 the Laplace operator. Equation (1) describes the static state.

In case of a time-dependent applied load and explicitly include inertia forces in the surface lateral loads according to d'Alambert's principle, then p and w are a function of time (Ventsel and Krauthammer, [12]). When forced vibrations $p(x,y,t)$ occur, a dynamic response of the plate with mass density ρ is produced. This leads to the following differential equation of forced, undamped motion of plates

$$D\nabla^2\nabla^2 w(x,y,t) = p(x,y,t) - \rho h\frac{\partial^2 w(x,y,t)}{\partial t^2}. \qquad (2)$$

Assuming that the plate is suddenly released from all external loads $(p(x,y,t)=0)$, the plate executes free or natural lateral vibrations which are functions of the material properties and the plate geometry. Then equation (2) can be written as

$$D\nabla^2\nabla^2 w(x,y,t) + \rho h\frac{\partial^2 w(x,y,t)}{\partial t^2} = 0. \qquad (3)$$

Mathematically exact solutions of the differential equation for the plate are extremely rare. They must on the one hand solve the differential equation and on the other hand meet the boundary conditions. Closed solutions are seldom available. In some cases the linearity of equation (1) allows a linear combination of the solutions in the form of a superposition. The general form of a strict solution of the differential equation can be specified in the following form

$$w(x,y) = w_H(x,y) + w_p(x,y). \qquad (4)$$

w_H is the homogeneous and w_p the particular solution of the inhomogeneous differential equation of the plate.

The solution for the freely vibrating plate is reduced to the solution of the homogeneous differential equation.

The natural frequencies and the corresponding mode shapes of the vibration (deflection surfaces in two dimensions) are of practical interest. Whereas the natural frequencies are the eigenvalues, the shape function represents the eigenfunctions. A general solution of equation (3) is

$$w(x,y,t) = (A\cos\omega t + B\sin\omega t)W(x,y), \quad (5)$$

where A and B are coefficients and $w(x,y,t)$ is a separable solution of the shape function $W(x,y)$ describing the modes of the vibration and some harmonic function of a time (Ventsel and Krauthammer, [12]). ω is the natural frequency of the plate got from the relationship $\omega = \frac{2\pi}{T}$ with T being the vibration period.

Using equation (5) the equation (3) is changed into

$$D\nabla^2\nabla^2 W(x,y) + \omega^2\rho h W(x,y) = 0. \quad (6)$$

The solution of equation (5) provides statements about the frequency spectrum of a plate. When m and n (with $m,n = 1,2,3,...$) are parameters denoting the number of harmonics along the x- and y-coordinate directions, respectively, the frequencies of a plate can be expressed by these parameters as ω_{mn}. The corresponding vibration mode shape function is $W_{mn}(x,y)$. In the case of a square, simply supported plate with edge length a, ω_{mn} can be calculated as

$$\omega_{mn} = \frac{\pi^2}{a^2}\left(m^2 + n^2\right)\sqrt{\frac{D}{\rho h}}. \quad (7)$$

For $m = 1$ and $n = 1$ the fundamental vibration frequency is obtained. The fundamental mode of flexural vibration is a single sine wave in the x and y direction. If m or n is equal to 2 and the other equal to 1, the next two higher modes are received. According to equation (7) these two modes have the same frequencies, but the associated mode shapes are different. The resulting vibration mode is a superimposition of these two modes taking account of any ratio of their maximum deflections. For a simply supported square plate with edge length a such a combination leads to the following shape function

$$W(x,y) = \sum_{m=1}^{\infty}\sum_{n=1}^{\infty} C_{mn}\sin\left(\frac{m\pi x}{a}\right)\sin\left(\frac{n\pi x}{a}\right), \quad (8)$$

where C_{mn} is the vibration amplitude for each value of m and n (Ventsel and Krauthammer, [12]).

The shown approximation is based on the Kirchhoff's plate theory (classical plate theory). It is necessary to draw attention to this point because the real vibration behavior which includes the deformation caused by transverse shear is not considered. An optimisation was done by the theories developed by Reissner [13] and Mindlin [14] whereas Mindlin improved the classical plate theory for plate vibrations by considering also the rotary inertia. It is not the aim of this work shown here to pick up different theories and to compare them. References can be made to the literature like e.g. Kant [15] and Reddy & Wang [16] dealing with this subject. An analytical treatment of the dynamic response of a rectangular clamped orthotropic plate subjected to a dynamic transverse moving load can for example be got from Alisjahbana [17]. However, it is striking that the focus in literature is mainly on the calculation of the frequency spectrum of a plate but not on the illustration of its vibrational pattern.

The presented work is targeted on the visualisation of the vibration behaviour of a clamped square plate using a sensitive sound localisation system. This should provide an indication of the real distribution of the nodal lines when an external force is applied. A calculation of the node lines for a rectangular plate with clamped edges is given by Soedel [18]. The node lines of a square plate clamped on all sides can be seen in Figure-8. It must be pointed out that this is the vibration pattern at the resonance frequencies. In our experiments the vibration modes are disturbed by the continuously applied external excitation and the variation of clamping conditions.

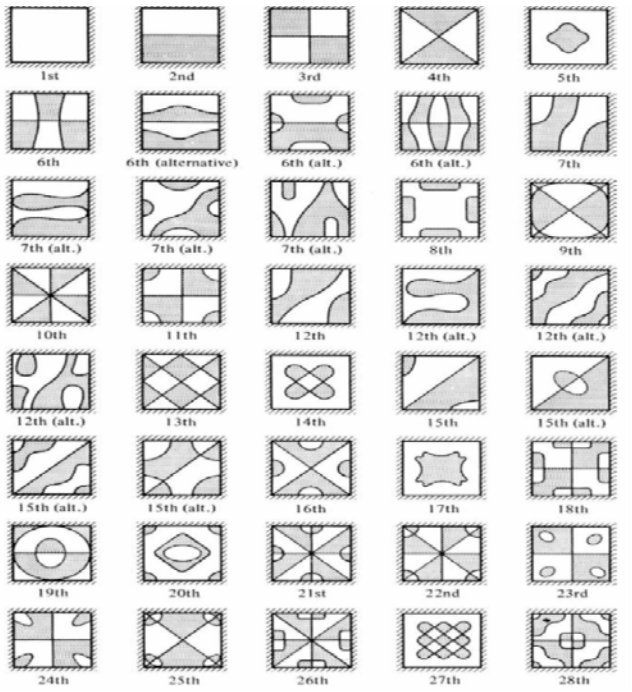

Figure-8. Some nodal patterns at different modes of vibration of square plates clamped on all edges (Szilard [19]).

3.2. Experimental studies of the Chladni figures

Figures-9 a) - 9 c) show the results of the Chladni experiment after a hammering of the lifting magnet for 30 minutes against the pane with a frequency of 20 Hz (Figure-9 a), 30 Hz (Figure-9 b) and 50 Hz (Figure-9 c). The blue circle in the center of each figure marks the position of the lifting magnet. The black crosses symbolize the bar clamps.

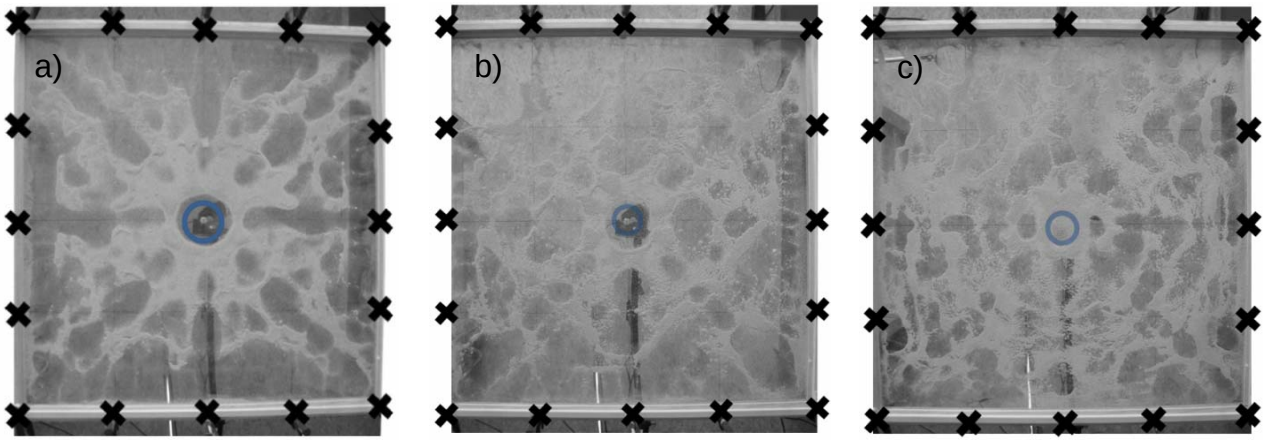

Figure-9. Chladni figures showing the nodal distribution of the oscillating acrylic glass pane for the following excitation frequencies: (a) 20 Hz, (b) 30 Hz and (c) 50 Hz.

It can be observed that even small differences between the excitation frequencies cause significant changes in the Chladni figures representing different vibration patterns. The areas in which the sand is sedimented demonstrate the nodal lines and, hence, the region where practically no vibration occurs. The higher the excitation frequency the more nodal lines develop. Furthermore, the acrylic glass pane is framed by sand which was expected because the bar clamps around the pane reduce the vibration.

The generated Chladni figures of Figures-9 a) - 9 c) are all quite symmetric (radial pattern). This effect can be attributed to the position of the lifting magnet which was placed in the center of the acrylic glass pane. The lifting magnet initiated a continuous excitation with a defined frequency and the corresponding oscillations of the pane forced the fine sand to concentrate on certain spots while those spots with high oscillation amplitudes stayed clear. In case of an excitation frequency of 20 Hz and 30 Hz the area where the lifting magnet touched the surface of the acrylic glass pane the sand moved away. At a frequency of 50 Hz this observation could not clearly confirmed. The tendency that the sand remains in the center of the pane with increasing excitation frequency can be estimated from the comparison between Figure-9 a) and Figure-9 b).

When bar clamps were removed the Chladni figure changed again, Figure-10. At the left half of the pane the Chladni figure is quite defined. Four lines that were confined by concentrated sand are clearly visible. At the right side of the pane these lines are not that distinct. Within a radius of about 10 - 15 cm taken from the center the pattern on the right side is specular with the left side. But at the fictitious line between the above and below removed clamps the symmetry begins to come apart. The sand does not form clear lines anymore but creates indefinable spots of concentration. Like in Figure-9 a) the sand stays at the left rim, but on the right edge the sand is missing, especially at the points where the bar clamps has been demounted.

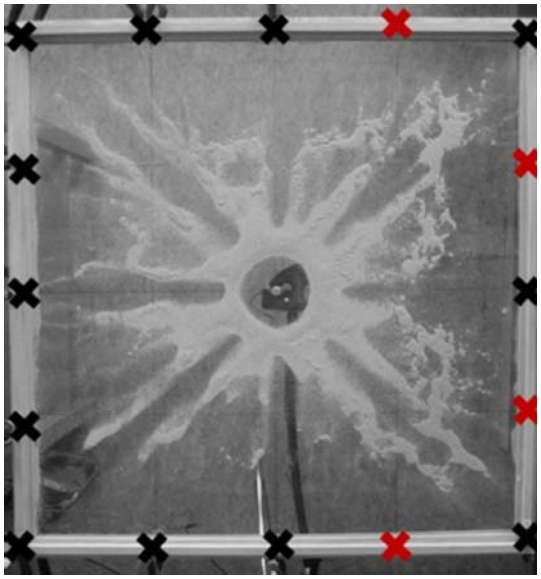

Figure-10. Chladni figure of the acrylic glass pane after removal of 4 bar clamps (marked by red crosses); excitation frequency: 20 Hz.

Based on this effect it can be concluded that the mounting (clamping condition) of the acrylic glass pane has a great influence on the distribution of vibrations that occur on plates. Compared to Figure-9 a) where the bar clamps were positioned in identical distances the equal distribution of vibration modes cannot be found here.

Figure-11 shows a completely different Chladni figure than Figure-9 a) or Figure-10 at an excitation

frequency of 20 Hz when two steel weights were put onto the pane. While before there were four clear lines free of sand only two lines arose now. There are also large areas free of sand at each side of the pane, except the rim where the sand is still present. The concentration of sand in the direct area around the steel weights is higher due to an additional mass at these zones which leads to a reduced vibration amplitude. Assuming that Chladni figures reflect the occurring vibrations it is clearly visible that these added objects disturb the whole oscillation behaviour. But against the background of a desired noise reduction of windows it can be assumed that a local stiffening of the used material is a possibility for a specific modification of the vibration behaviour.

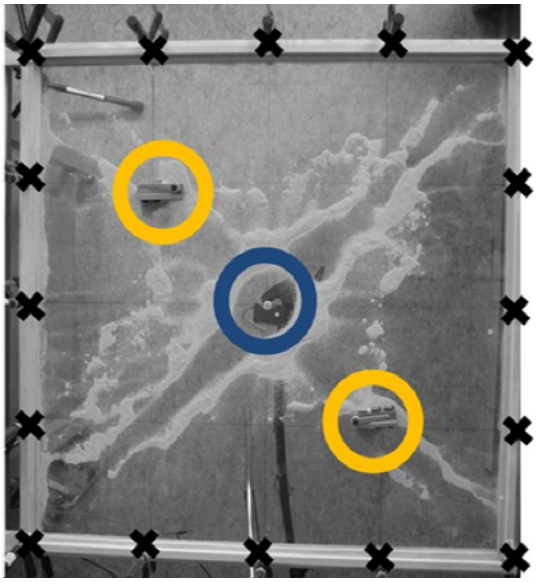

Figure-11. Chladni figure of the acrylic glass pane using all bar clamps (marked by black crosses) but additional masses (yellow circles); excitation frequency: 20 Hz.

The Chladni figure that is shown in Figure-12 is the result of another position of the lifting magnet. In the area around the lifting magnet close to the wooden mounting laths strong vibrations occur because this zone is free of sand. The rest of the acrylic glass pane is covered by sand that forms many small empty spots all over the pane. An almost mirror-symmetric pattern can be found along the diagonal between the upper left corner and the bottom right corner where the lifting magnet is positioned. The remaining spots seem to be arrayed in circles around the lifting magnet.

The resulting Chladni pattern serves as a good example of how the location of the excitation influences the vibrations of the acrylic glass pane. When the lifting magnet was positioned in the center of the pane the Chladni figure spreads out radially around it. If it is positioned at the corner as seen in Figure-12 there still is certain symmetry but the distribution of vibrations is completely different. The comparison between the results of Figure-12 and Figure-9 c) suggests that in case of the shifting of the lifting magnet a denser vibration pattern develops as it occurs when a higher excitation frequency is applied. It is striking that despite strong clamping the edges are not heavily coated with sand being contrary to the classical plate theory with clamped edges.

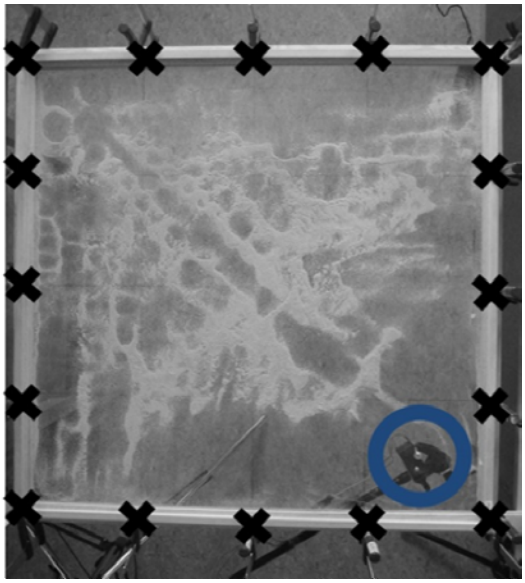

Figure-12. Chladni figure of the acrylic glass pane using all bar clamps (marked by black crosses) but shifted lifting magnet (blue circle); excitation frequency: 20 Hz.

3.3. Recognition of the received vibration pattern using a Microflown™ probe

After removal of the sand the acoustic measurements using the sound localisation system (Microflown™ probe) were carried out under the same experimental conditions like described for the determination of the nodal lines. The resulting images have been made slightly transparent and laid upon the previously created images of the sand figures (Figure-13). This allows a good comprehension of both results.

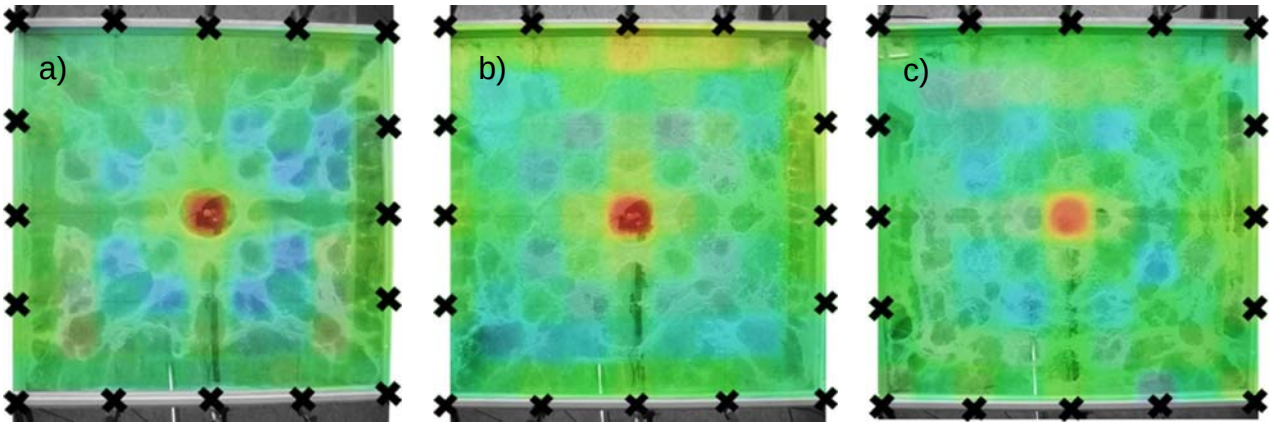

Figure-13. Overlaid acoustic figures showing the measured particle velocity of the vibrating acrylic glass pane for the following excitation frequencies: a) 20 Hz, b) 30 Hz and c) 50 Hz.

The different particle velocity is a result of the local sound emission. The data of every measurement checkpoint is set in relation with data of all other checkpoints within the measurement. The highest value of particle velocity is colour-coded in red; the lowest particle velocity is colour-coded in blue. Additional colours are also possible whereas the whole colour scale is equal to that known from an infrared camera. In respect of this procedure the vibration pattern of the acrylic glass pane should be made visible and the nodal lines be estimated.

The matching with the sand figures representing the Chladni figures shows that the highest particle velocity occurs in the center of the pane (Figure-13) which is attributable to the hammering of the lifting magnet. Only in case for the excitation frequency of 50 Hz a weaker signal can be measured. It is expected that the sand remains in the center which was seen in Figure-9 c). The edges where all bar clamps are mounted lead to a bluish colour (Figure-13 a, excitation frequency: 20 Hz) which means that this area does not carry out strong transversal vibrations. Thus, these zones should be covered with sand which was observed (Figure-9 a). The blue coloured areas are predominantly in accordance with the sandy sectors. At an excitation frequency of 30 Hz (Figure-13 b) only the areas with a lot of sand can be considered as in compliance with the blue zones of the acoustic measurements. Areas with no sand are mainly green coloured. The center of the pane seems to be more vibrating than other regions but the sand is still present. It is assumed that the sand reacts very slowly to changes of the vibration modes. The vibration pattern at an excitation frequency of 50 Hz (Figure-13 c) is different from that one received at 30 Hz. A reduced oscillation occurs in the center of the pane and areas with low vibration amplitudes are observable in a region 20 - 25 cm from the midpoint of the pane. Again, like in Figure-13 a) blue fields arise at the edges where a higher concentration of sand (Figure-9 c) has been deposited. The sand can show the nodal lines but the acoustic measurements give a hint on the amplitude of the vibration for a special place.

When four bar clamps were removed (Figure-14) the vibration pattern is not anymore as dendritic as seen in Figure-9 a). The blue areas are in good accordance with the sand deposits and the edges are more vibrating, especially in the upper and right edge. The demounting of some bar clamps appears to be sufficient to change the vibrating structure significantly.

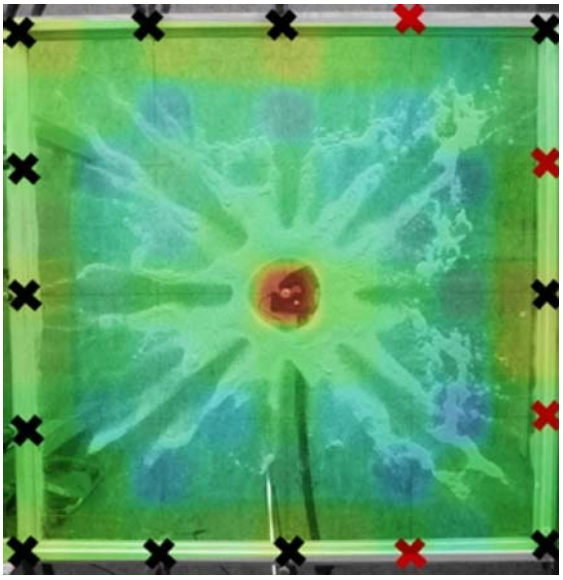

Figure-14. Overlaid acoustic figure of the acrylic glass pane after removal of 4 bar clamps (marked by red crosses); excitation frequency: 20 Hz.

As seen in Figure-11 two steel weights were put on the acrylic glass pane. The corresponding acoustic measurement at an excitation frequency of 20 Hz is shown in Figure-15. The place of each weight can be determined by the dark blue or purple coloured area. In the direction of the center a more vibrating zone is observable. Larger sand deposits correspond with bluish coloured zones. Especially, the effect of mounting of the glass pane in the corners is clearly visible by the acoustic measurements. These areas do not seem to oscillate in contrast to the neighboring areas. It must therefore be assumed that the region near the frame was excited into oscillation due to putting the weights on the acrylic glass pane.

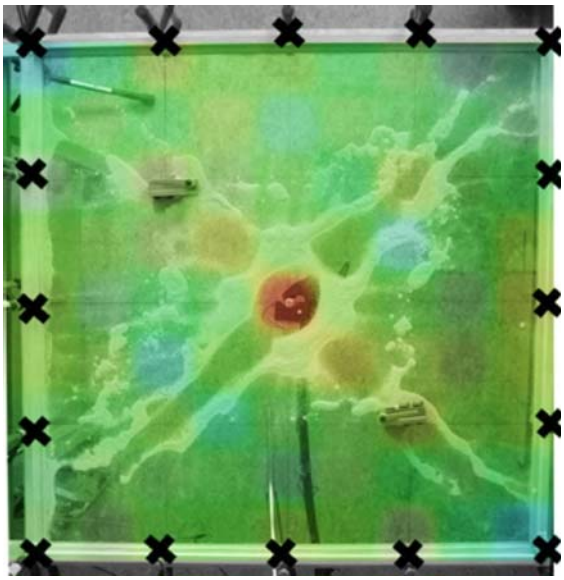

Figure-15. Overlaid acoustic figure of the acrylic glass pane using all bar clamps (marked by black crosses) but additional masses; excitation frequency: 20 Hz.

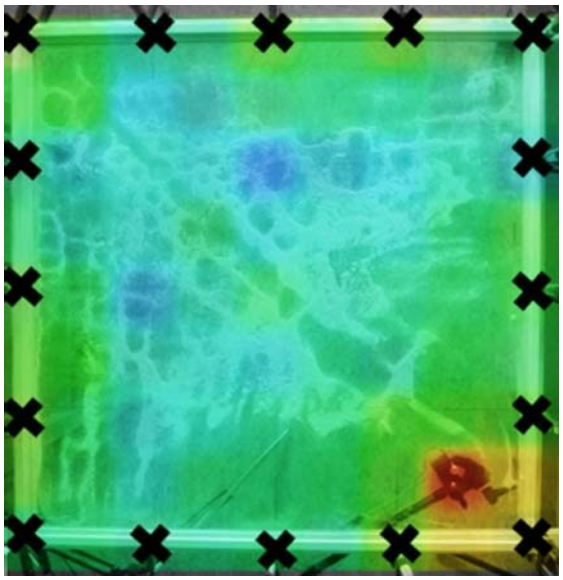

Figure-16. Overlaid acoustic figure of the acrylic glass pane using all bar clamps (marked by black crosses) but shifted lifting magnet; excitation frequency: 20 Hz.

A relocation of the excitation point which is shown in Figure-16 led to a shift of the area colour-coded in red. It can be noted that a detection of the maximum oscillation amplitude is clearly possible using the Microflown™ probe. The sand distribution along the diagonal from the upper left corner and the low right corner is symmetric and the corresponding blue marked areas are as well. According to Figure-12 only a very low amount of sand is deposited near the rims (e.g. the upper edge). The acoustic measurements show that vibrations should occur because this area is not colour-coded in blue but mainly in yellowish green. An exact correlation between the acoustic measurements and the small areas without sand cannot be determined because the acoustic data were taken from particle velocity measurements which proved to be sensitive to further mechanical vibrations like frame oscillations. However, due to the shown acoustic measurements a rough estimation of the vibration pattern of the acrylic glass pane can be made. Therefore, targeted technical measures can be carried out to suppress critical vibration amplitudes and to realize an increase in comfort for the crew and passengers on a ship.

4. CONCLUSIONS

The common way for obtaining the vibration pattern of a plate is by determining its nodal lines. This can be done by mathematical calculations or by experiments using fine-grained sand in order to produce Chladni figures. The mathematical solutions suffer from the exact boundary conditions meaning a precise consideration of the clamping and excitation conditions. Furthermore, the experiments with sand are often time-consuming and cannot be performed when the plate stands upright.

The purpose of the experiment was to present an alternative contact-free method to visualise oscillations of a plate (colour-coded pictures of an acrylic glass pane) due to an external force in order to test it as a measurement method for the investigation of oscillating parts like glass panes on a ship. Three different excitation frequencies (20 Hz, 30 Hz and 50 Hz) generated by a lifting magnet were applied. By using a sound source localisation system (Microflown™ probe) it was possible to determine the excitation point and to get a vibrating pattern of this pane. The vibrating pattern was compared with Chladni figures received by sand deposits and obtained under the same experimental conditions. A good correlation between the acoustic image and the Chladni figures could be obtained at an excitation frequency of 20 Hz. With increasing frequency the sand was more distributed and a complex vibration pattern was observed. The accordance between the colour-coded acoustic results and the sand pattern was sometimes very inadequate, especially at higher frequencies.

At an excitation frequency of 20 Hz some bar clamps mounted at the edges of the pane were removed. The vibration pattern changed and the oscillation at the edges seemed to increase. Generally, zones with no sand deposit could be recognized as vibrating areas. It could be

observed that the mounting of the acrylic glass pane appeared to have a great influence on the results of the acoustic measurement and the Chladni figures, respectively. When the missing bar clamps were mounted again additional weights were laid on the acrylic glass pane. Dark blue or purple-coloured fields got from the acoustic measurements developed around the position of the weights. In this area the sand was sedimented, too. The Chladni figure only consisted of a few but distinctive lines. A more complex figure was received when the position of the lifting magnet was shifted. The excitation point could clearly be detected as well as the areas which should strongly vibrate. These areas are characterized by missing or barely existing sand deposits.

In summary it can be stated that there was no locally precise accordance between the Chladni figures and the visualised acoustic data. Nevertheless, at least qualitative assessments of the vibration pattern are possible so that technical changes can purposefully be carried out to vibrating objects like glass panes in order to decrease the noise level or to avoid critical vibration amplitudes.

ACKNOWLEDGEMENT

Prof. Dr. Jürgen Göken gratefully acknowledges the financial support of the German Research Foundation (DFG, www.dfg.de; DFG-reference number: INST 21572/1-1 LAGG) for the sound localisation system. The acoustic measurements were done within the framework of the project “MariTIM” (Interreg IV A-Programme between Germany and the Netherlands being co-financed by the European Regional Development Fund (EFRE)). Prof. Dr. Jürgen Göken would like to take this opportunity to thank this funding programme for its financial support.

REFERENCES

[1] Germanischer Lloyd Aktiengesellschaft. 2009. Rules for classification and construction. I Ship technology: ch. 23, p. 1.

[2] Asmussen I., W. Menzel and H. Mumm. 2001. Ship vibration. GL Technology: p. 7.

[3] Göken J. 2013. Result of acoustic measurements in the framework of the Interreg IV A-project “MariTIM” (INTERREG-Programme of the European Union); www.maritim-de-nl.eu (Accessed on 10 April 2014).

[4] Microflown™. 2012. Manual PU-regular (V1.0 2012 - 07), www.microflown.com (Accessed on 9 April 2014).

[5] Ma C.-C. and H.-L. Lin. 2005. Experimental measurements on transverse vibration characteristics of piezoceramic rectangular plates by optical methods. J. Sound Vib. 286: 587-600.

[6] Chladni E.F.F. 1787. Entdeckungen über die Theorie des Klanges. Weidmanns Erben und Reich, Leipzig.

[7] Bergmann L., C. Schaefer and H. Gobrecht. 1974. Lehrbuch der Experimentalphysik, vol. 1: Mechanik, Akustik, Wärme. Walter de Gruyter and Co. pp. 525-528.

[8] Balasubramanian A. 2001. Plate analysis with different geometries and arbitrary boundary conditions. University of Texas at Arlington, Master´s thesis.

[9] Tomotika S. 1936. The transverse vibration of a square plate clamped at four edges. Phil. Mag. S. 7. 21: 745-760.

[10] Leissa A.W. 1969. Vibration of plates. Scientific and Technical Information Division, National Aeronautics and Space Administration.

[11] Göken J., J. Swiostek, H. Hurdelbrink and U. Keil. 2013. Acoustic measurements for determination of the materials damping using a sound source localisation system. Acta Metall. Sin. (Engl. Lett.) 26(2): 113-121.

[12] Ventsel E. and T. Krauthammer. 2001. Thin plates and shells - Theory, analysis, and applications. Marcel Dekker, Inc. ch. 9.

[13] Reissner E. 1954. The Effect of transverse shear deformation on the bending of elastic plates. J. Appl. Mech. 12: A69-A77.

[14] Mindlin R.D. 1951. Influence of rotatory inertia and shear on flexural motions of isotropic elastic plates. J. Appl. Mech. 18: 31-38.

[15] Kant T. 1982. Numerical analysis of thick plates. Comput. Meth. Appl. Mech. Eng. 31(1): 1-18.

[16] Reddy J.N., C.M. Wang. 1997. Relationships between classical and shear deformation theories of axisymmetric circular plates. AIAA J. 35(12): 1862-1868.

[17] Alisjahbana S.W. 2004. Dynamic response of clamped orthotropic plates to dynamic moving loads. 13th World Conference on Earthquake Engineering, Vancouver, B.C., Canada.

[18] Soedel W. 2004. Vibrations of shells and plates (3rd edition). Marcel Dekker, Inc. p. 90.

[19] Szilard R. 2004. Theories and applications of plate analysis - Classical, numerical and engineering methods. John Wiley and Sons, Inc. p. 807.